

1

2 Investigation of the extreme wet-cold compound events changes between 2025-2049 and  
3 1980-2004 using regional simulations in Greece

4 Iason Markantonis<sup>1,2</sup>, Diamando Vlachogiannis<sup>1</sup>, Athanasios Sfetsos<sup>1</sup>, Ioannis Kioutsioukis<sup>2</sup>

5 <sup>1</sup>Environmental Research Laboratory, NCSR “Demokritos”, 15341 Agia Paraskevi, Greece

6 <sup>2</sup>University of Patras, Department of Physics, University Campus 26504 Rio, Patras, Greece

7 *Correspondence to:* Iason Markantonis (jasonm@ipta.demokritos.gr)

8 **Abstract.** This paper aims to study wet-cold compound events (WCCEs) in Greece for the wet and  
9 cold season November-April, since these events may affect directly human activities for short or longer  
10 periods as no similar research has been conducted for the country studying the past and future  
11 development of these compound events. WCCEs are divided in two different daily compound events  
12 (Maximum Temperature (TX) -Accumulated Precipitation (RR)) and (Minimum Temperature (TN) –  
13 Accumulated Precipitation (RR)) using fixed thresholds (RR over 20 mm/day and Temperature under 0  
14 °C). Observational data from the Hellenic National Meteorology Service (HNMS) and simulation data  
15 from reanalysis and EURO-CORDEX models were used in the study for the historical period 1980-  
16 2004. The Ensemble mean of the simulation datasets from projection models were employed for the  
17 near future period (2025-2049) to study the impact of climate change on the occurrence of WCCEs  
18 under the Representative Concentration Pathways (RCPs) 4.5 and 8.5 scenarios. Following data  
19 processing and validation of the models, the potential changes in the distribution of WCCEs in the  
20 future were investigated based on the projected and historical simulations. WCCEs determined by fixed  
21 thresholds were mostly found over high altitudes with TN-RR events exhibiting a future tendency to  
22 reduce particularly under RCP 8.5 scenario and TX-RR exhibiting similar reduction of probabilities for  
23 both scenarios.

24

## 25 1. Introduction

26 Extreme weather events and their linkage to climate change is a matter of high concern for many  
27 scientific groups (Zanocco et al., 2018; Konisky et al., 2016; Curtis et al., 2017). In the last decade,  
28 numerous scientific studies focused on the causes, the frequency and impacts of extreme compound  
29 events (e.g. Aghakouchak et al., 2020; Singh et al., 2021; Sadegh et al., 2018; Zscheischler et al., 2017;  
30 Zscheischler and Seneviratne, 2017; Zscheischler et al., 2018). As mentioned in the Intergovernmental  
31 Panel on Climate Change report on “Managing the risks of extreme events and disasters to advance  
32 climate change adaptation” (IPCC SREX) (Ref 7, p. 118) compound events are defined as: (1) two or  
33 more extreme events occurring simultaneously or successively, (2) combinations of extreme events  
34 with underlying conditions that amplify the impact of the events, or (3) combination of events that are  
35 not themselves extremes but lead to an extreme event or impact when combined (Leonard et al., 2014).

36 Recent studies have been conducted on the examination of wet-cold compound events (WCCEs) that  
37 concern daily values of temperature and precipitation and the correlation of these variables  
38 (Chukwudum and Nadarajah, 2022; Lhotka and Kyselý, 2021) , while other studies focus on the  
39 occurrence of monthly WCCEs for the historical period (Wu et al., 2019; Lemus-Canovas, 2022)  
40 However, the purpose of this article is the study of fixed thresholds extreme WCCEs on daily basis in  
41 Greece during the historical period (1980-2004) and how the likelihood of these events will be affected  
42 by climate change, during the period 2025-2049. It has been reported that WCCEs affect the region of  
43 the Mediterranean Basin, including Greece (Zhang et al., 2021). Studies using only observational data  
44 at some locations (Lazoglou and Anagnostopoulou, 2019), or modeled data mostly over the broader  
45 region of the Mediterranean Sea (Vogel et al., 2021; Hochman et al., 2021; de Luca et al., 2020),  
46 concerning WCCEs have been conducted in the past, but not depicting analytically WCCEs in Greece,  
47 a country that as a part of the Mediterranean Basin is considered a “Climate change hotspot” (Ali et al.,  
48 2022.) . This work attempts to fill this void on the effects of climate change on WCCEs in Greece.

49 The examined events belong to the first category of the definition of compound events from IPCC  
50 since they refer to the simultaneous exceedance of precipitation and temperature thresholds. WCCEs  
51 may have a negative impact on people's lives by causing electricity blackouts, affecting agriculture  
52 with heavy snowfall or freezing rain and blocking transportation because of closed roads, railways or  
53 even airports (Houston et al., 2006; Llasat et al., 2014; Vajda et al., 2014). On the other hand, most of  
54 the available freshwater in the country comes from melted mountain snow during spring or summer.  
55 Finally, eco-systems, especially in mountains, may be affected by the absence of snow that climate  
56 change may cause (Demiroglu et al., 2015; Pestereva et al., 2012; Trujillo et al., 2012; García-Ruiz et  
57 al., 2011).

58 The first part of the study concerns the historical period between 1980 and 2004, because of the  
59 availability of quality controlled daily observational data for minimum temperature (TN), maximum  
60 temperature (TX) and accumulated precipitation (RR). Hence, for that period, we use observational  
61 data from 21 Hellenic National Meteorological Service (HNMS) stations, to validate EURO-CORDEX  
62 Regional Climate Models (RCMs), provided by the Copernicus Climate Change Service and the  
63 projection model dataset produced in-house. In addition to the models, two reanalysis products are  
64 included, as the closest to "true" past climate conditions in regions with no or scarce observations  
65 (Moalafhi et al., 2016). More information about the observational and model datasets is presented in  
66 Section 2. Section 3 highlights the applied methodology while Section 4 displays WCCEs observed in  
67 stations and station cells of the models and Section 5 contains reanalysis and projections Ensemble  
68 mean WCCEs probabilities spatial distribution for the historical period. Section 6 details the results  
69 about the difference in WCCEs probabilities between the historical and the near future period between  
70 2025 and 2049 for two greenhouse gas concentration scenarios, RCP 4.5 and RCP 8.5.

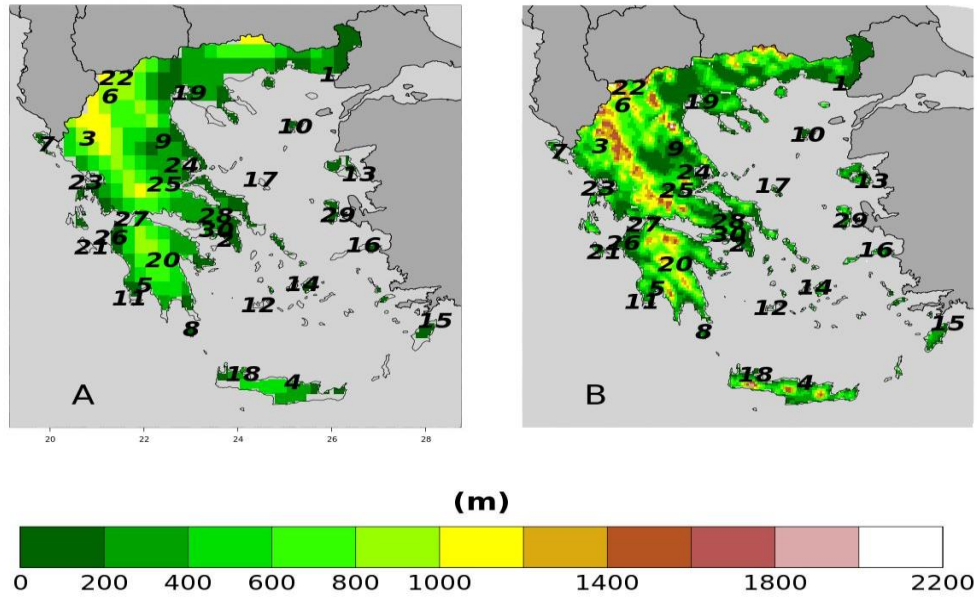
## 71 **2. Data**

72 In this Section, we present the datasets that provide the observational and simulation data produced by  
73 projection and reanalysis models.

### 74 **1. HNMS observations**

75 HNMS provides freely observational data from 21 stations for the purpose of scientific research  
76 (<http://www.emy.gr/emv/el/services/paroxi-ipiresion-elfthera-dedomena>). The data have been  
77 formally evaluated by HNMS and the timeseries show no missing or distorted values. In particular, the  
78 timeseries available for the historical period 1980-2004 have a 3-hour temporal resolution and from  
79 these values we have extracted the daily values of TN, TX and RR. Moreover, stations 22-30 that also  
80 belong in the network of HNMS stations contain observations in the period 1980-2004, although none  
81 of the stations covers all observational days in the period. The datasets of these stations were extracted  
82 by National Centers for Environmental Information of National Oceanic and Atmospheric  
83 Administration. We selected stations that contain at least 20 years of observations. Figure 1 shows the  
84 position of the stations on the orography of ERA5 and WRF, while Table A1 of Appendix provides  
85 details on the characteristics of the stations. We have used the observational data to validate the model  
86 datasets regarding the WCCEs for the historical period.

87



88

89 **Figure 1: Map of HNMS stations on orography of (A) ERA5 and (B) WRF-ERAinterim. The**  
 90 **numbers correspond to those in Table A1 (Appendix).**

91 **2.2 Reanalysis models**

92 We have used two reanalysis models due to the lack of spatially and temporally complete direct  
 93 observations, to study more consistently the WCCes in Greece in the historical period. The first model  
 94 is the latest available reanalysis product ERA 5 from the European Centre for Medium-Range Weather  
 95 Forecasts (ECMWF) of spatial resolution  $\sim 30\text{km} \times 30\text{km}$  (Hersbach et al., 2020). The second  
 96 reanalysis model, built in the Environmental Research Laboratory (EREL) of National Center of  
 97 Scientific Research ‘Demokritos’ (NCSR) WRF\_ERA\_I, has been produced by dynamically  
 98 downscaling ERA-INTERIM using the Weather Research Forecast (WRF) model (v3.6.1) from  $80\text{km} \times$   
 99  $80\text{km}$  to  $5\text{km} \times 5\text{km}$  (Politi et al., 2021, 2020, 2018).

100 **2.3 GCM / RCM models**

101 To observe possible alterations of WCCes occurrence probability in the future period 2025-2049  
 102 compared to the historical period, we employed data from RCM simulations driven by GCMs. In this  
 103 regard, we obtained data from 5 models included in the EURO-CORDEX initiative provided by the  
 104 Copernicus Program. All chosen EURO-CORDEX models with available daily data for both RCP  
 105 scenarios were selected because they have the finest spatial resolution of  $0.11^\circ \times 0.11^\circ$ , and have also  
 106 been tested in Cardoso et al, (2019). Information on the regional and parent models and their acronyms  
 107 used herewith is given in Table 1. In addition to the EURO-CORDEX model data, we have used  
 108 dynamically downscaled data from the EC-EARTH GCM to high spatial resolution of  $5\text{km} \times 5\text{km}$  for  
 109 the area of Greece using the WRF model (Politi et al., 2020, 2022).

Institution	Reference	Regional Model	Forcing model	Acronym	Resolution ( $^\circ$ )
Météo-France / Centre National de Recherches Météorologiques	(Spiridonov et al., n.d.)	ALADIN63	CNRM- CERFACS- CNRM-CM5	CNRM	0.11
Koninklijk Nederlands Meteorologisch Instituut	(van Meijgaard et al., 2008)	KNMI- RACMO22E	ICHEC-EC- EARTH	KNMI	0.11

<b>Climate Limited-Area Modelling Community</b>	(Rockel et al., 2008)	CLMcom-CLM-CCLM4-8-17	MOHC-HadGEM2-ES	CLMcom	0.11
<b>Swedish Meteorological and Hydrological Institute</b>	(Samuelsson et al., 2016)	SMHI-RCA4	MPI-M-MPI-ESM-LR	SMHI	0.11
<b>Danish Meteorological Institute</b>	(Christensen, 2006)	DMI-HIRHAM5	NCC-NorESM1-M	DMI	0.11
<b>EREL (NCSRD)</b>	(Politi et al. 2020, 2022)	ARW-WRF	EC-EARTH	WRF_EC	0.05

110

111 **Table 1: EURO-CORDEX and EREL-NCSRD simulation models information.**

112

113

### 3. Methodology

114

The first step in this study is the validation of the projection and reanalysis models against observations. Moreover, the ensemble of the 6 projection models is also exhibited. We choose as the Ensemble resolution that of the CORDEX models since 5 of them share the same spatial resolution. The only model in need of regridding is WRF\_EC. We follow the nearest neighbor method to upscale WRF\_EC from 5 km to 11 km. In addition, we use box-plots to depict the ability of the models to simulate observational data WCCEs probabilities for the historical period at the cells that include meteorological stations. The box-plots consist of the colored box, where in the band near the middle of the box is the median, the bottom and top of each color box are the 25<sup>th</sup> (Q1) and 75<sup>th</sup> (Q3) percentiles (BL) percentile. The lower limit of the whisker (LLW) is calculated by  $LLW = Q1 - 1.5 * BL$  and the upper limit (ULW) by  $ULW = Q3 + 1.5 * BL$ . The length of the whiskers (WL) is calculated as the difference between ULW and LLW. Any value out of this range is marked by a black point in the plot. The validation is conducted after the elevation bias correction of temperature at the cells of the models containing the stations. The cells of the stations are found using the nearest neighbor approach and the temperature bias correction temperature is the following:

115

$$T_s = T_m + 0.006 * (H_m - H_s) \quad (1)$$

116

In equation (1),  $T_s$  is the temperature of the cell after the elevation bias correction,  $T_m$  the temperature provided by the model,  $H_m$  the cell elevation and  $H_s$  the elevation of the HNMS station.

117

#### 3.1 Compound event selection

118

According to HNMS, the meteorological year can be split into two climate periods (<http://emy.gr/emy/el/climatology/climatology>). The cold and wet period extends on average from mid-October to the end of March, and the warm-dry period occurs during the rest of the year. Since the study is focused on the extreme WCCEs, we examine the period between November and April, since according to the HNMS observations, April exhibits lower temperatures than October and more rainy days. Moreover, it is not uncommon for the northern parts of Greece, and especially mountainous areas, to be affected by snowfalls during April. This leads to the creation of a timeseries of 4532 daily values for the historical period and 4531 for the future period. CLMcom considers that each month is consisted by 30 days, thus leading to 4500 values for each period. Also, DMI considers that a calendar year has 365 days, thus each period examined has 4525 values.

119

The WCCEs, which are examined on daily basis, are divided in two types of synchronous events, TX-RR and TN-RR and studied using the fixed threshold approach (Table 2). This approach considers the fixed threshold of 20 mm/day for RR and 0 °C for TN and TX for all stations or grid points, as recommended by the Commission for Climatology (CCI), the World Climate Research Programme (WCRP) of the Climate Variability and Predictability Component (CLIVAR) project and the Expert

120

121

122

123

124

125

126

147 Team for Climate Change Detection and Indices (ETCCDI). TN equal to or under 0 °C indicates Frost  
 148 Days (FD), while TX equal to or under 0 °C Iced Days (ID) (Fonseca et al., 2016). The thresholds  
 149 examined have been proposed in various works for studying extreme events (Raziei et al., 2014; Tošić  
 150 and Unkašević, 2013; Anagnostopoulou and Tolika, 2012; Pongrácz et al., 2009; Kundzewicz et al.,  
 151 2006; Moberg et al., 2006)..

THRESHOLDS	RR	TN	TX	WCCE	
FIXED	$\geq 20$ mm/day (RR20)	$\leq 0$ °C (FD)	$\leq 0$ °C (ID)	1.	(RR20-FD)
				2.	(RR20-ID)

152

153 **Table 2: Univariate thresholds and the compound events examined in the study.**

154 **3.2 WCCEs probability calculation**

155 The WCCEs probabilities are calculated by applying two different methods. The first is the empirical  
 156 approach counting the events from the timeseries and dividing by the total number of days to find the  
 157 percentage (%) of the occurrence probability. For the second method, we use the copula approach for  
 158 the HNMS observations and model comparison and to map the differences between the two methods  
 159 for the reanalysis and projection of model data. Compared to copula, an empirical method has a higher  
 160 uncertainty when calculating the probability of extreme events (Hao et al., 2018; Tavakol et al., 2020;  
 161 Zscheischler and Seneviratne, 2017). The purpose of using two different methods is to investigate  
 162 whether the copula method underestimates or overestimates the WCCEs.

163 The best fitting copula selection for each timeseries is examined using the R programming language  
 164 function BiCopSelect as suggested in (Zhou et al., 2019)(Zhou et al., 2019)(Zhou et al., 2019)(Zhou et al.,  
 165 2019)(Zhou et al., 2019)(Zhou et al., 2019)(Zhou et al., 2019)(Zhou et al., 2019)(Zhou et al., 2019)(Zhou et al.,  
 166 2019)(Zhou et al., 2019)(Zhou et al., 2019)(Zhou et al., 2019)(Zhou et al., 2019) package VineCopula  
 167 (Schepsmeier et al., 2013). The appropriate bivariate copula for each dataset is chosen by the function,  
 168 from a multitude of 40 different copula families using the Akaike Information Criterion (AIC) (Akaike,  
 169 1974) and Bayesian Information Criterion (BIC) , and the copula chosen for each station and model  
 170 dataset is shown in Appendix B (Tables B1 and B2). Copulas are used in plenty of studies that  
 171 investigate the dependence between two different climate variables and the joint probability of  
 172 compound events (Tavakol et al., 2020; Dzupire et al., 2020; Pandey et al., 2018; Cong and Brady,  
 173 2012; Abraj and Hewaarachchi, 2021).

174 As mentioned in Nelsen, (2007), a bivariate copula is a bivariate distribution function where margins  
 175 are uniform on the unit interval [0, 1]. A bivariate copula is a map  $C:[0,1]^2 \rightarrow [0,1]$  with  $C(u,1)=u$  and  
 176  $C(1,v)=v$ . Let  $X$  and  $Y$  be random variables with a joint distribution function  $F(x,y)=Pr(X \leq x, Y \leq y)$  and  
 177 continuous marginal distribution functions  $F_1(x)=Pr(X \leq x)$  and  $F_2(y)=Pr(Y \leq y)$ , respectively. By Sklar's  
 178 theorem (Sklar, 1959), one obtains a unique representation

179 
$$F(x,y) = C\{F_1(x),F_2(y)\} \tag{2}$$

180 For the two random variables of  $X$  (e.g., precipitation) and  $Y$  (e.g., temperature) with cumulative  
 181 distribution functions (CDFs)  $F_1(x)=Pr(X \geq x)$  and  $F_2(y)=Pr(Y \leq y)$ , the bivariate joint distribution  
 182 function or copula ( $C$ ) can be written as:

183 
$$F(x,y) =Pr(X \geq x, Y \leq y) = C(u,v) \tag{3}$$

184 **4. WCCEs assessment in HNMS stations**

185 In this section, the models are validated against observations both for the empirical and the copula  
 186 method. WCCEs probabilities for each station and model are presented in the supplementary material.  
 187 BIAS and RMSE along with the Critical Success Index (CSI) are used for the validation. CSI is  
 188 calculated as:  $CSI=A/(A+B+C)$ .  $A$ ,  $B$  and  $C$  symbolize elements from the contingency table (Table 2)  
 189 that occur from comparing zero and non-zero probabilities in stations with the corresponding model  
 190 cells. Also, total number of events calculated for both methods from observational data are presented in  
 191 each station.

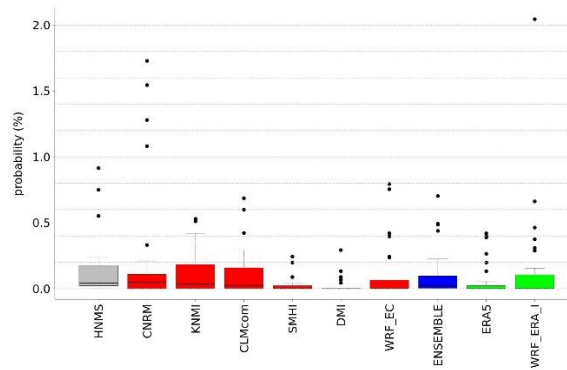
"EVENT"=POSITIVE PROBABILITY		OBSERVATION EVENT	
		YES	NO
MODEL EVENT	YES	<b>A</b>	<b>B</b>
	NO	<b>C</b>	<b>D</b>

192 **Table 2: Contingency table where "A" is the number of event forecasts that correspond to event**  
193 **observations, or the number of hits. Entry "B" is the number of event forecasts that do not**  
194 **correspond to observed events, or the number of false alarms. Entry "C" is the number of no-**  
195 **event forecasts corresponding to observed events, or the number of misses. Entry "D" is the**  
196 **number of no-event forecasts corresponding to no events observed, or the number of correct**  
197 **rejections.**

198 **4.1 RR20FD**

199 Probability values for each station are presented in Supplementary (Tables S1-S4) as well as the  
200 contingency tables (Tables S7-S10) from which CSI is calculated. ERA5 and WRF\_ERA\_I are  
201 reanalysis products and exhibited for comparison reasons. The copulas selected by Bicopselect for each  
202 observational and modeled timeseries are also presented in Supplementary (Tables S5-S6).

203

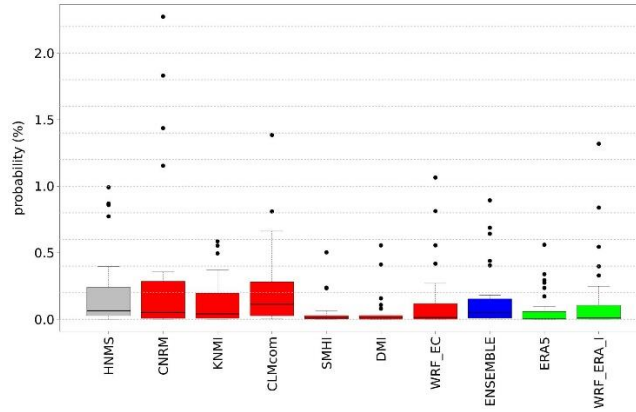


204

205 **Figure 2: Box-plot presenting RR20FD empirical method probabilities for observations and**  
206 **models.**

	<i>HNMS</i>	<i>CNRM</i>	<i>KNMI</i>	<i>CLMcom</i>	<i>SMHI</i>	<i>DMI</i>	<i>WRF_EC</i>	<i>ENSEMBLE</i>	<i>ERA5</i>	<i>WRF_ERA_I</i>
<i>MEAN</i>	<b>0.1382</b>	0.2361	0.1168	0.1116	0.0267	0.0208	0.1143	<b>0.1044</b>	0.0625	0.1535
<i>SD</i>	<b>0.2211</b>	0.4821	0.1590	0.1781	0.0581	0.0600	0.2216	<b>0.1813</b>	0.1311	0.3935
<i>BIAS</i>		-0.0979	0.0214	0.0266	0.1115	0.1174	0.0239	<b>0.0338</b>	0.0756	-0.0154
<i>RMSE</i>		0.3234	0.1298	0.0922	0.2003	0.2148	0.1222	<b>0.0975</b>	0.1536	0.2319
<i>COR</i>		0.8583	0.8138	0.9211	0.9194	0.7177	0.8484	<b>0.9118</b>	0.8210	0.8523
<i>CSI</i>		0.6071	0.6667	0.6296	0.3214	0.1667	0.3793	<b>0.7692</b>	0.2667	0.4483

207 **Table 3: Table exhibiting mean (MEAN) station RR20FD empirical probabilities (%) for**  
208 **observations and models, standard deviation (SD), bias (BIAS), rmse (RMSE), Pearson**  
209 **correlation (COR) and CSI of models against observations.**



210

211 **Figure 3: Box-plot presenting RR20FD copula method probabilities for observations and models.**

	<i>HNMS</i>	<i>CNRM</i>	<i>KNMI</i>	<i>CLMcom</i>	<i>SMHI</i>	<i>DMI</i>	<i>WRF_EC</i>	<i>ENSEMBLE</i>	<i>ERA5</i>	<i>WRF_ERA_I</i>
<i>MEAN</i>	<b>0.2016</b>	0.2974	0.1291	0.2129	0.0448	0.0528	0.1338	<b>0.1451</b>	0.0699	0.1455
<i>SD</i>	<b>0.2864</b>	0.5802	0.1715	0.3031	0.1042	0.1237	0.2580	<b>0.2310</b>	0.1368	0.2939
<i>BIAS</i>		-0.0959	0.0725	-0.0113	0.1568	0.1488	0.0678	<b>0.0565</b>	0.1317	0.0561
<i>RMSE</i>		0.3334	0.1720	0.2264	0.2646	0.2530	0.1458	<b>0.1139</b>	0.2165	0.1788
<i>COR</i>		0.9422	0.8782	0.6968	0.7688	0.7620	0.8888	<b>0.9467</b>	0.8955	0.8233
<i>CSI</i>		0.9259	0.9629	1	0.9643	0.7333	0.8276	<b>1</b>	0.6333	0.7931

212

213 **Table 4: Table exhibiting mean (MEAN) RR20FD copula station probabilities (%) for**  
 214 **observations and models, standard deviation (SD), bias (BIAS), rmse (RMSE), Pearson**  
 215 **correlation (COR) and CSI of models against observations.**

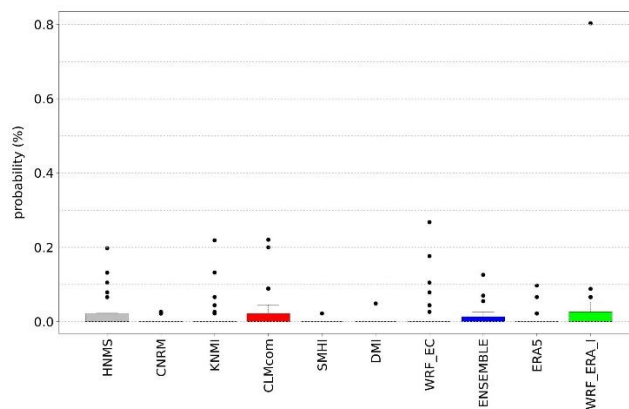
216

#### 4.2 RR20ID

217

218 RR20ID events yield, as expected, lower probabilities than RR20FD events as observed in Figures 4  
 219 and 5. Most observations and models yield zero probabilities, hence validation of models for these  
 220 events is limited. The empirical method exhibits eight stations stations with non-zero probabilities in  
 221 the historical period (Supplementary).

222



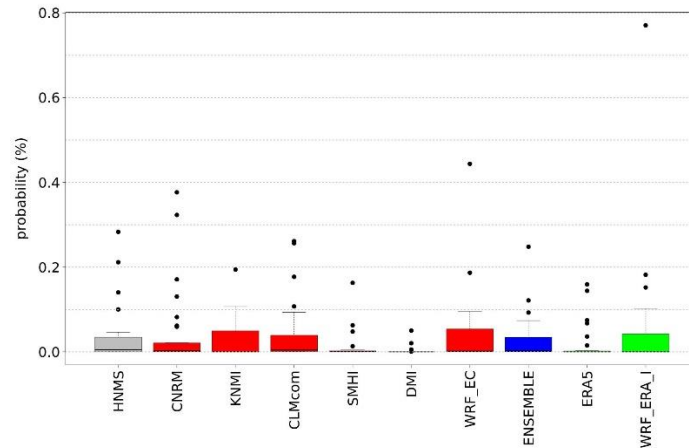
223

224 **Figure 4: Box-plot presenting RR20ID empirical method probabilities for observations and**  
 225 **models.**

*HNMS* *CNRM* *KNMI* *CLMcom* *SMHI* *DMI* *WRF\_EC* *ENSEMBLE* *ERA5* *WRF\_ERA\_I*

<i>MEAN</i>	<b>0.0331</b>	0.0430	0.0240	0.0397	0.0104	0.0029	0.0388	<b>0.0265</b>	0.0167	0.0493
<i>SD</i>	<b>0.0669</b>	0.0933	0.0440	0.0725	0.0320	0.0098	0.0876	<b>0.0524</b>	0.0413	0.1441
<i>BIAS</i>		-0.0099	0.0091	-0.0065	0.0228	0.0303	-0.0057	<b>0.0067</b>	0.0164	-0.0161
<i>RMSE</i>		0.0568	0.0466	0.0556	0.0522	0.0682	0.0636	<b>0.0419</b>	0.0438	0.1084
<i>COR</i>		0.7961	0.7212	0.6780	0.7506	0.5380	0.6829	<b>0.7776</b>	0.8101	0.6928
<i>CSI</i>		0.1071	0.2000	0.1923	0.0333	0.0333	0.1481	<b>0.2400</b>	0.1034	0.1538

225 **Table 5: Table exhibiting mean (MEAN) RR20ID empirical probabilities station probabilities**  
 226 **(%) for observations and models, standard deviation (SD), bias (BIAS), rmse (RMSE), Pearson**  
 227 **correlation (COR) and CSI of models against observations.**



228

229 **Figure 5: Box-plot presenting RR20ID copula method probabilities for observations and models.**

	<i>HNMS</i>	<i>CNRM</i>	<i>KNMI</i>	<i>CLMcom</i>	<i>SMHI</i>	<i>DMI</i>	<i>WRF_EC</i>	<i>ENSEMBLE</i>	<i>ERA5</i>	<i>WRF_ERA_I</i>
<i>MEAN</i>	<b>0.0282</b>	0.0378	0.0169	0.0344	0.0066	0.0017	0.0249	<b>0.0204</b>	0.0138	0.0274
<i>SD</i>	<b>0.0663</b>	0.0811	0.0303	0.0676	0.0166	0.0046	0.0473	<b>0.0364</b>	0.0377	0.0524
<i>BIAS</i>		-0.0097	0.0112	-0.0062	0.0215	0.0264	0.0032	<b>0.0078</b>	0.0144	0.0008
<i>RMSE</i>		0.0532	0.0493	0.0598	0.0565	0.0691	0.0489	<b>0.0443</b>	0.0420	0.0339
<i>COR</i>		0.7534	0.7228	0.5861	0.8202	0.2291	0.6594	<b>0.7712</b>	0.8370	0.8540
<i>CSI</i>		0.5000	0.4333	0.8095	0.5357	0.2667	0.5000	<b>0.8095</b>	0.2667	0.4286

230 **Table 6: Table exhibiting mean (MEAN) RR20ID copula probabilities station probabilities (%)**  
 231 **for observations and models, standard deviation (SD), bias (BIAS), rmse (RMSE), Pearson**  
 232 **correlation (COR) and CSI of models against observations.**

### 233 4.3 Observations-models comparison conclusions

234 The events examined are rare among the available stations for the historical period. Copulas  
 235 considering the dependence between the variables yield greater probabilities than the empirical method.  
 236 More stations with non-zero probabilities enable more accurate validation of the models. To minimize  
 237 uncertainties, smooth extreme underestimations or overestimations of WCCE probabilities that each  
 238 model yields, and because ENSEMBLE shows better consistency among the projection models'  
 239 statistical indices, we use it for further analysis in the study.

## 240 5. Historical period models WCCEs on maps

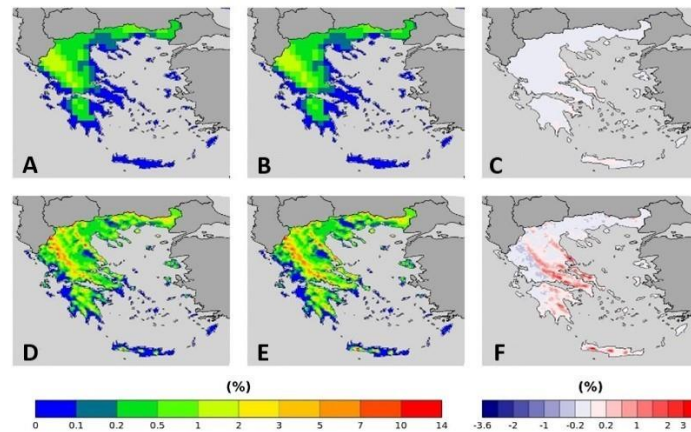
241 In this section, WCCEs spatial distribution probabilities are compared between empirical and copula  
 242 methods. This procedure is conducted separately for the two reanalysis products and the Ensemble  
 243 mean of the projection models.



244 **5.1 Reanalysis**

245 ERA5 and WRF\_ERA\_I WCCEs spatial distribution probabilities in Greece are displayed in this  
 246 section. We display both reanalysis products, although ERA5 is the most recently developed reanalysis  
 247 product, we exhibit also WRF\_ERA\_I since its much finer spatial resolution is more appropriate for the  
 248 complex topography of Greece with many mountains and islands.

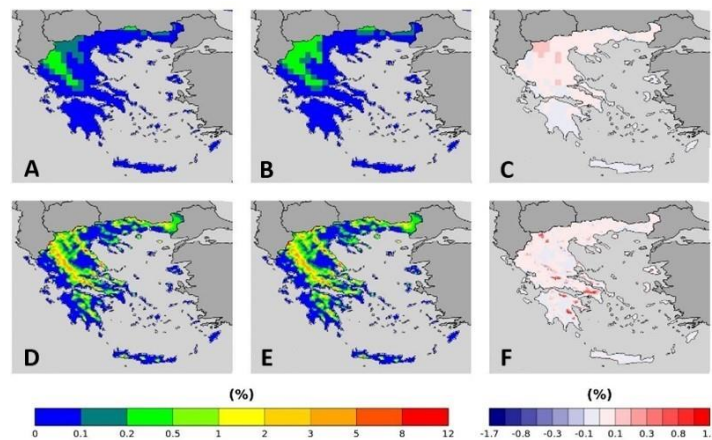
249



250

251 **Figure 6: RR20FD probabilities for (A, B, C) ERA5 and (D, E, F) WRF\_ERA\_I produced by (A,**  
 252 **D) Empirical and (B, E) Copula and (C) = (B)–(A) and (F)=(E)-(D).**

253



254

255 **Figure 7: RR20ID probabilities for (A, B, C) ERA5 and (D, E, F) WRF\_ERA\_I produced by**  
 256 **(A,D) Empirical and (B, E) Copula and (C) = (B)–(A) and (F) = (E)-(D).**

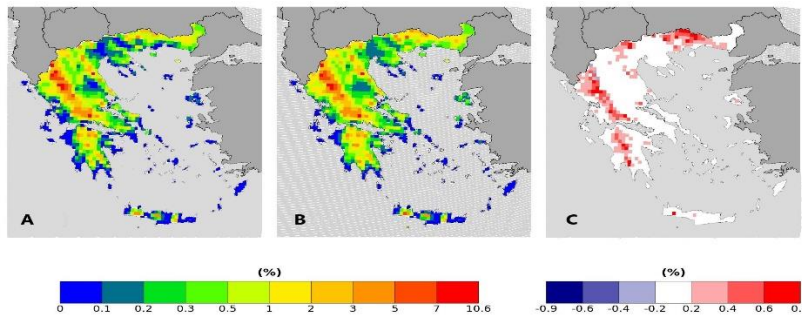
257 Both reanalysis products yield greater WCCEs probabilities in the Pindus mountains, although due to  
 258 its finer spatial resolution, WRF\_ERA\_I display high probabilities at other mountainous regions  
 259 located in Crete, Peloponnese, Evia Island and others. Also, in both WCCEs copula method yields  
 260 higher probabilities, especially for WRF\_ERA\_I and the RR20FD case. Moreover, WRF\_ERA\_I  
 261 displays a greater range than ERA5 with RR20FD probabilities reaching 14% and RR20ID 12%  
 262 compared to 6% and 2% of ERA5 respectively.

263 **5.2 Projections Ensemble**

264 Figures 8 and yield that the Ensemble mean displays similar to WRF\_ERA\_I spatial distribution of  
 265 WCCEs. RR20FD and RR20ID probabilities reach 10.8% and 5.4% respectively. The copula method  
 266 yields higher probabilities for both methods in mountainous regions with greater difference displayed

267 for RR20ID events in the Pindos mountain range and RR20FD exhibiting greater spatial distribution in  
 268 differences between the two methods.

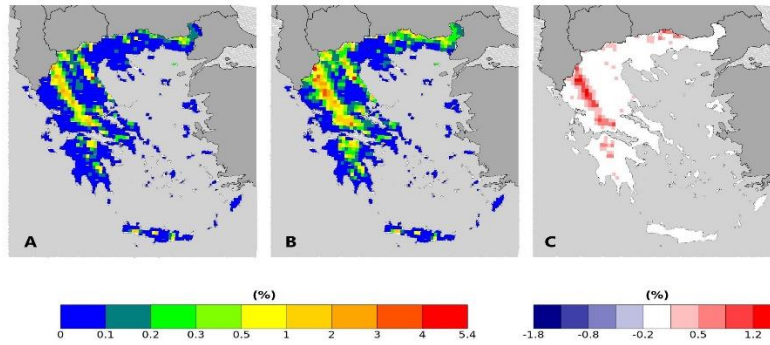
269



270

271 **Figure 8: RR20FD Ensemble probabilities for (A) Empirical and (B) Copula method. (C)=(B)-**  
 272 **(A).**

273



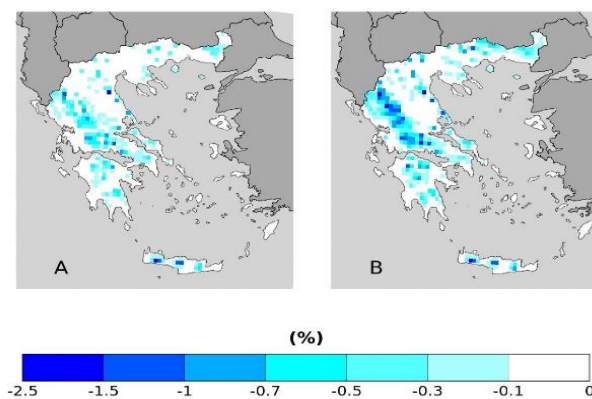
274

275 **Figure 9: RR20ID Ensemble probabilities for (A) Empirical and (B) Copula method. (C)=(B)-(A).**

276 **6. Past-Future Ensemble differences**

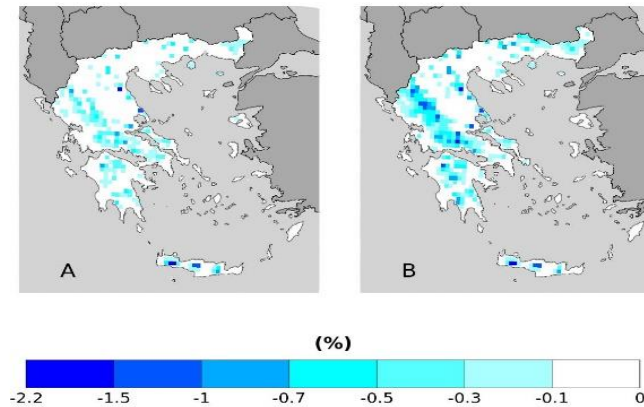
277 This section displays the differences of the Ensemble mean WCCes probabilities, calculated for the  
 278 empirical and the copula method, compared to the past probabilities presented in the previous section.  
 279 The differences mapped are statistically significant at a 95% level using the Student's t-test (Goulden,  
 280 1939) comparing 25 annual values of the timeseries.

281 **6.1 RR20FD**



282

283 **Figure 10: RR20FD empirical method probability differences of future-past periods for (A)**  
 284 **RCP4.5 and (B) RCP8.5 scenarios.**



285

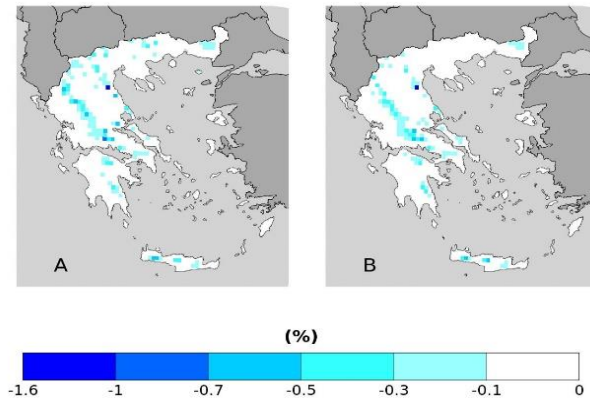
286 **Figure 11: RR20FD copula method probability differences of future-past periods for (A) RCP4.5**  
 287 **and (B) RCP8.5 scenarios.**

	<i>Empirical RCP4.5</i>	<i>Empirical RCP8.5</i>	<i>Copula RCP4.5</i>	<i>Copula RCP8.5</i>
$0 \leq N_c < 0.1$	34	31	64	57
$-0.1 \leq N_c < -0.3$	112	154	112	131
$-0.3 \leq N_c < -0.5$	63	65	53	81
$-0.5 \leq N_c < -0.7$	31	48	16	47
$-0.7 \leq N_c < -1$	12	34	6	24
$-1 \leq N_c < -1.5$	5	18	3	11
$N_c \leq -1.5$	2	5	3	4
<i>MAX D</i>	-1.8063 %	-2.4988 %	-1.9500 %	-2.1392 %

288 **Table 7: ENSEMBLE Number of cells (Nc) in each category of probability difference (%) for**  
 289 **RR20FD for empirical and copula method. MAX D denotes the maximum negative difference**  
 290 **between future and past periods. Nv concerns only cells with statistically significant difference.**

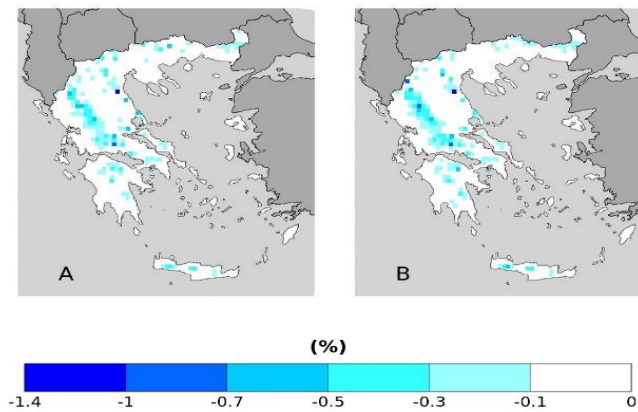
291 From the results displayed in Figures 10 and 11 and in Table 7 RCP4.5 and RCP8.5 scenarios for the  
 292 probabilities of the RR20FD events we observe that in all cases future scenarios yield only negative  
 293 values, meaning the reduction of RR20FD events in 2025-2049 period compared to 1980-2004 period  
 294 in all mountainous regions of Greece. RCP8.5 yields greater reduction of RR20FD probabilities than  
 295 the RCP4.5 scenario both in spatial distribution and extreme values. The empirical method exhibits a  
 296 greater reduction for the RCP8.5 scenario, although for the RCP4.5 scenario both methods yield similar  
 297 results.

298 **6.2 RR20ID**



299

300 Figure 12: RR20ID empirical method probability differences of future-past periods for (A)  
 301 RCP4.5 and (B) RCP8.5 scenarios.



302

303 Figure 13: RR20ID copula method probability differences of future-past periods for (A) RCP4.5  
 304 and (B) RCP8.5 scenarios.

	<i>Empirical RCP4.5</i>	<i>Empirical RCP8.5</i>	<i>Copula RCP4.5</i>	<i>Copula RCP8.5</i>
$0 \leq N_c < -0.1$	193	229	166	210
$-0.1 \leq N_c < -0.3$	81	71	96	109
$-0.3 \leq N_c < -0.5$	23	20	33	37
$-0.5 \leq N_c < -0.7$	9	5	9	7
$-0.7 \leq N_c < -1$	1	0	1	3
$N_c \leq -1$	1	1	1	1
<i>MAX D</i>	-1.5536	-1.0593	-1.3425	-1.1362

305 Table 8: ENSEMBLE Number of cells ( $N_c$ ) in each category of probability difference (%) for  
 306 RR20ID for empirical and copula method. MAX D denotes the maximum negative difference  
 307 between future and past periods.  $N_v$  concerns only cells with statistically significant difference.

308 Similarly, to RR20FD, RR20ID events probabilities yield only zero or negative differences compared  
 309 to the past for both scenarios. Empirical and copula methods yield similar results in distribution and  
 310 extreme values. For both methods, the RCP4.5 scenario tends to higher reduction of RR20ID  
 311 probabilities than RCP8.5, as observed in Table 8.

312 The results for both scenarios and events show that independently from the choice of scenario, the  
 313 probabilities of the events are expected to reduce almost equally in the near future (2025-2049)  
 314 compared to the past period (1980-2004).

This work presents for the first time to our knowledge an extensive study of wet-cold compound events in Greece for the historical and future periods of 1980-2004 and 2025-2049, respectively. Models' data from the EUROCORDEX initiative of 0.11° resolution and reanalysis data (ERA5 and ERA-Interim dynamically downscaled to 5km<sup>2</sup>) were used and validated for the determined WCCEs against the formally available observational datasets by HNMS for the country. The number of events and their probabilities of occurrence were determined by applying a fixed thresholds approach. Then, the bivariate validation of the models' datasets against observations was performed for the determined bivariate thresholds. The probabilities of WCCEs were computed using the empirical method and the best-fitted copula for the bivariate timeseries for observational data, reanalysis, projection models and the Ensemble of the projection models. Copulas yield higher extreme events probabilities for most of the cases considering the dependence between temperature and precipitation

. Although, uncertainties may rise on the impact of WCCEs on mountainous areas due to the absence of observations on altitudes higher than 1000 meters, we trust the results yielded by the Ensemble. Besides the satisfying results from the bivariate validation, this trust is enhanced by the fact that winter period systems affect large areas crossing the country from north to south or from west to east (Cartalis et al., 2010) and therefore recorded by available stations. Also, in the cold period of the year, convective precipitation forced by orography is limited hence the doubt that the models do not simulate extreme rainfall in winter is reduced. Moreover, the use of the Ensemble mean of the models reduces the uncertainties on models' ability to simulate the probability of occurrence of extreme events occurrences. The reduction of RR20-FD and RR20-ID WCCEs on mountains that the Ensemble of projection models predict in the future, might contribute to less heavy snowfall events and possibly less accumulated snow depth. If such a scenario will be verified, Greece faces the threat of losing the main sources of fresh water that come from melted mountain snow during spring or early summer in the near future period. The rise of temperature due to global warming is the main factor for the reduction of WCCEs (Supplementary Figures S5-S7), while also possible changes in patterns of teleconnections may affect winter conditions in Greek mountains, similar to NAO (North Atlantic Oscillation) pattern affecting Pindos mountains (López-Moreno et al., 2011) or the positive phase of EAWR (East Atlantic-Western Russia) pattern that leads to cold air advection from the north towards the southern part of Europe and eastern Mediterranean region (Ionita, 2014). Still, understanding of extreme events on complex terrains demands greater effort from the scientific community to enable solid predictions on the impact of climate change on the occurrence of these events.

#### 347 Acknowledgments

The authors acknowledge partial funding by the project "National Research Network for Climate Change and its Impacts, (CLIMPACT - 105658/17-10-2019)" of the Ministry of Development, GSRT, Program of Public Investment, 2019.

#### 351 References

- 352 Abdi, H.: The Kendall Rank Correlation Coefficient, 2007.
- 353 Abraj, M. A. M. and Hewaarachchi, A. P.: Joint return period estimation of daily maximum and  
354 minimum temperatures using copula method, 66, 175–190, <https://doi.org/10.17654/AS066020175>,  
355 2021.
- 356 Aghakouchak, A., Chiang, F., Huning, L. S., Love, C. A., Mallakpour, I., Mazdiyasni, O., Moftakhari,  
357 H., Papalexiou, S. M., Ragno, E., and Sadegh, M.: Climate Extremes and Compound Hazards in a  
358 Warming World, 48, 519–548, <https://doi.org/10.1146/ANNUREV-EARTH-071719-055228>, 2020.
- 359 Akaike, H.: A New Look at the Statistical Model Identification, 19, 716–723,  
360 <https://doi.org/10.1109/TAC.1974.1100705>, 1974.
- 361 Ali, E., Cramer, W., Carnicer, J., Georgopoulou, E., Hilmi, N. J. M., le Cozannet, G., Lionello, P.,  
362 Pörtner, H.-O., Roberts, D. C., Tignor, M., Poloczanska, E. S., Mintenbeck, K., Alegría, A., Craig, M.,

363 Langsdorf, S., Löschke, S., Möller, V., Okem, A., and Rama, B.: SPM 2233 CCP4 Mediterranean  
364 Region to the Sixth Assessment Report of the Intergovernmental Panel on Climate Change [, 2233–  
365 2272, <https://doi.org/10.1017/9781009325844.021>, n.d.

366

367 Anagnostopoulou, C. and Tolika, K.: Extreme precipitation in Europe: Statistical threshold selection  
368 based on climatological criteria, 107, 479–489, [https://doi.org/10.1007/S00704-011-0487-  
369 8/TABLES/2](https://doi.org/10.1007/S00704-011-0487-8/TABLES/2), 2012.

370 Balkema, A. A. and Haan, L. de: Residual Life Time at Great Age, 2, 792–804,  
371 <https://doi.org/10.1214/AOP/1176996548>, 1974.

372 Cartalis, C., Chrysoulakis, N., Feidas, H., and Pitsitakis, N.: International Journal of Remote Sensing  
373 Categorization of cold period weather types in Greece on the basis of the photointerpretation of  
374 NOAA/AVHRR imagery Categorization of cold period weather types in Greece on the basis of the  
375 photointerpretation of NOAA/AVHRR imagery, <https://doi.org/10.1080/01431160310001632684>,  
376 2010.

377 Cardoso, R. M., Soares, P. M. M., Lima, D. C. A., and Miranda, P. M. A.: Mean and extreme  
378 temperatures in a warming climate: EURO CORDEX and WRF regional climate high-resolution  
379 projections for Portugal, 52, 129–157, <https://doi.org/10.1007/S00382-018-4124-4/FIGURES/8>, 2019.

380 Christensen, O. B.: Regional climate change in Denmark according to a global 2-degree-warming  
381 scenario, 2006.

382 Chukwudum, Q. C. and Nadarajah, S.: Bivariate Extreme Value Analysis of Rainfall and Temperature  
383 in Nigeria, *Environmental Modeling and Assessment*, 27, 343–362, [https://doi.org/10.1007/S10666-  
384 021-09781-7/TABLES/13](https://doi.org/10.1007/S10666-021-09781-7/TABLES/13), 2022.

385 Coles, S.: An Introduction to Statistical Modeling of Extreme Values, [https://doi.org/10.1007/978-1-  
386 4471-3675-0](https://doi.org/10.1007/978-1-4471-3675-0), 2001.

387 Cong, R. G. and Brady, M.: The interdependence between rainfall and temperature: Copula analyses,  
388 2012, <https://doi.org/10.1100/2012/405675>, 2012.

389 Curtis, S., Fair, A., Wistow, J., Val, D. v., and Oven, K.: Impact of extreme weather events and climate  
390 change for health and social care systems, 16, 23–32, [https://doi.org/10.1186/S12940-017-0324-  
391 3/METRICS](https://doi.org/10.1186/S12940-017-0324-3/METRICS), 2017.

392 de Luca, P., Messori, G., Faranda, D., Ward, P. J., and Coumou, D.: Compound warm-dry and cold-wet  
393 events over the Mediterranean, 11, 793–805, <https://doi.org/10.5194/ESD-11-793-2020>, 2020.

394 Demiroglu, O. C., Kučerová, J., and Ozcelebi, O.: Snow reliability and climate elasticity: Case of a  
395 Slovak ski resort, 70, 1–12, <https://doi.org/10.1108/TR-01-2014-0003/FULL/PDF>, 2015.

396 Dzupire, N. C., Ngare, P., and Odongo, L.: A copula based bi-variate model for temperature and  
397 rainfall processes, 8, e00365, <https://doi.org/10.1016/J.SCIAF.2020.E00365>, 2020.

398 Fisher, R. A. and Tippett, L. H. C.: Limiting forms of the frequency distribution of the largest or  
399 smallest member of a sample, 24, 180–190, <https://doi.org/10.1017/S0305004100015681>, 1928.

400 Fonseca, D., Carvalho, M. J., Marta-Almeida, M., Melo-Gonçalves, P., and Rocha, A.: Recent trends of  
401 extreme temperature indices for the Iberian Peninsula, 94, 66–76,  
402 <https://doi.org/10.1016/J.PCE.2015.12.005>, 2016.

403 García-Ruiz, J. M., López-Moreno, I. I., Vicente-Serrano, S. M., Lasanta-Martínez, T., and Beguería,  
404 S.: Mediterranean water resources in a global change scenario, 105, 121–139,  
405 <https://doi.org/10.1016/J.EARSCIREV.2011.01.006>, 2011.

406 Gilleland, E. and Katz, R. W.: extRemes 2.0: An Extreme Value Analysis Package in R, 72, 1–39,  
407 <https://doi.org/10.18637/JSS.V072.I08>, 2016.

408 Gnedenko, B.: Sur La Distribution Limite Du Terme Maximum D’Une Serie Aleatoire, 44, 423,  
409 <https://doi.org/10.2307/1968974>, 1943.

410 Goda, Y.: Inherent Negative Bias of Quantile Estimates of Annual Maximum Data Due to Sample Size  
411 Effect: A Numerical Simulation Study, 53, 397–429, <https://doi.org/10.1142/S0578563411002409>,  
412 2018.

413 Goulden, C.: Methods of statistical analysis., 1939.

414 Hao, Z., Singh, V. P., and Hao, F.: Compound Extremes in Hydroclimatology: A Review, 10, 718,  
415 <https://doi.org/10.3390/W10060718>, 2018.

416 Hersbach, H., Bell, B., Berrisford, P., Hirahara, S., Horányi, A., Muñoz-Sabater, J., Nicolas, J., Peubey,  
417 C., Radu, R., Schepers, D., Simmons, A., Soci, C., Abdalla, S., Abellan, X., Balsamo, G., Bechtold, P.,  
418 Biavati, G., Bidlot, J., Bonavita, M., de Chiara, G., Dahlgren, P., Dee, D., Diamantakis, M., Dragani,  
419 R., Flemming, J., Forbes, R., Fuentes, M., Geer, A., Haimberger, L., Healy, S., Hogan, R. J., Hólm, E.,  
420 Janisková, M., Keeley, S., Laloyaux, P., Lopez, P., Lupu, C., Radnoti, G., de Rosnay, P., Rozum, I.,  
421 Vamborg, F., Villaume, S., and Thépaut, J. N.: The ERA5 global reanalysis, 146, 1999–2049,  
422 <https://doi.org/10.1002/QJ.3803>, 2020.

423 Hochman, A., Marra, F., Messori, G., Pinto, J., Raveh-Rubin, S., Yosef, Y., and Zittis, G.: ESD  
424 Reviews: Extreme Weather and Societal Impacts in the Eastern Mediterranean, 1–53,  
425 <https://doi.org/10.5194/ESD-2021-55>, 2021.

426 Houston, T. G., Changnon, S. A., Ae, T. G. H., and Changnon, S. A.: Freezing rain events: a major  
427 weather hazard in the conterminous US, 40, 485–494, <https://doi.org/10.1007/S11069-006-9006-0>,  
428 2006.

429 Ionita, M.: The Impact of the East Atlantic/Western Russia Pattern on the Hydroclimatology of Europe  
430 from Mid-Winter to Late Spring, *Climate 2014*, Vol. 2, Pages 296-309, 2, 296–309,  
431 <https://doi.org/10.3390/CLI2040296>, 2014.

432 James Pickands: Statistical Inference Using Extreme Order Statistics, 3, 119–131,  
433 <https://doi.org/10.1214/AOS/1176343003>, 1975.

434 Konisky, D. M., Hughes, L., and Kaylor, C. H.: Extreme weather events and climate change concern,  
435 134, 533–547, <https://doi.org/10.1007/S10584-015-1555-3/FIGURES/3>, 2016.

436 Kundzewicz, Z. W., Radziejewski, M., and Pińskwar, I.: Precipitation extremes in the changing climate  
437 of Europe, 31, 51–58, <https://doi.org/10.3354/CR031051>, 2006.

438 Lazoglou, G. and Anagnostopoulou, C.: Joint distribution of temperature and precipitation in the  
439 Mediterranean, using the Copula method, 135, 1399–1411, [https://doi.org/10.1007/S00704-018-2447-  
440 Z/FIGURES/5](https://doi.org/10.1007/S00704-018-2447-Z/FIGURES/5), 2019.

441 Lemus-Canovas, M.: Changes in compound monthly precipitation and temperature extremes and their  
442 relationship with teleconnection patterns in the Mediterranean, *Journal of Hydrology*, 608, 127580,  
443 <https://doi.org/10.1016/J.JHYDROL.2022.127580>, 2022.

444 Leonard, M., Westra, S., Phatak, A., Lambert, M., van den Hurk, B., McInnes, K., Risbey, J., Schuster,  
445 S., Jakob, D., and Stafford-Smith, M.: A compound event framework for understanding extreme  
446 impacts, 5, 113–128, <https://doi.org/10.1002/WCC.252>, 2014.

447 Lhotka, O. and Kysely, J.: Precipitation–temperature relationships over Europe in CORDEX regional  
448 climate models, *International Journal of Climatology*, <https://doi.org/10.1002/JOC.7508>, 2021.

449 Llasat, M. C., Turco, M., Quintana-Seguí, P., and Llasat-Botija, M.: The snow storm of 8 March 2010  
450 in Catalonia (Spain): a paradigmatic wet-snow event with a high societal impact, 14, 427–441,  
451 <https://doi.org/10.5194/NHESS-14-427-2014>, 2014.

452 López-Moreno, J. I., Vicente-Serrano, S. M., Morán-Tejeda, E., Lorenzo-Lacruz, J., Kenawy, A., and  
453 Beniston, M.: Effects of the North Atlantic Oscillation (NAO) on combined temperature and  
454 precipitation winter modes in the Mediterranean mountains: Observed relationships and projections for  
455 the 21st century, *Glob Planet Change*, 77, 62–76,  
456 <https://doi.org/10.1016/J.GLOPLACHA.2011.03.003>, 2011.

457 Markantonis, I., Vlachogiannis, D., Sfetsos, T., Kioutsioukis, I., and Politi, N.: An Investigation of  
458 cold-wet Compound Events in Greece, <https://doi.org/10.5194/EMS2021-188>, 2021.

459 Moalafhi, D. B., Evans, J. P., and Sharma, A.: Evaluating global reanalysis datasets for provision of  
460 boundary conditions in regional climate modelling, 47, 2727–2745, <https://doi.org/10.1007/S00382-016-2994-X/TABLES/9>, 2016.

462 Moberg, A., Jones, P. D., Lister, D., Walther, A., Brunet, M., Jacobeit, J., Alexander, L. v., Della-  
463 Marta, P. M., Luterbacher, J., Yiou, P., Chen, D., Tank, A. M. G. K., Saladié, O., Sigró, J., Aguilar, E.,  
464 Alexandersson, H., Almarza, C., Auer, I., Barriendos, M., Begert, M., Bergström, H., Böhm, R., Butler,  
465 C. J., Caesar, J., Drebs, A., Founda, D., Gerstengarbe, F. W., Micela, G., Maugeri, M., Österle, H.,  
466 Pandzic, K., Petrakis, M., Srnec, L., Tolasz, R., Tuomenvirta, H., Werner, P. C., Linderholm, H.,  
467 Philipp, A., Wanner, H., and Xoplaki, E.: Indices for daily temperature and precipitation extremes in  
468 Europe analyzed for the period 1901–2000, 111, 22106, <https://doi.org/10.1029/2006JD007103>, 2006.

469 Nelsen, R.: An introduction to copulas, 2007.

470 Pandey, P. K., Das, L., Jhajharia, D., and Pandey, V.: Modelling of interdependence between rainfall  
471 and temperature using copula, 4, 867–879, <https://doi.org/10.1007/S40808-018-0454-9>, 2018.

472 Pestereva, N. M., Popova, N. Yu., and Shagarov, L. M.: Modern Climate Change and Mountain Skiing  
473 Tourism: the Alps and the Caucasus, 1602–1617, 2012.

474 Politi, N., Nastos, P. T., Sfetsos, A., Vlachogiannis, D., and Dalezios, N. R.: Evaluation of the AWR-  
475 WRF model configuration at high resolution over the domain of Greece, 208, 229–245,  
476 <https://doi.org/10.1016/J.ATMOSRES.2017.10.019>, 2018.

477 Politi, N., Sfetsos, A., Vlachogiannis, D., Nastos, P. T., and Karozis, S.: A Sensitivity Study of High-  
478 Resolution Climate Simulations for Greece, 8, 44, <https://doi.org/10.3390/CLI8030044>, 2020.

479 Politi, N., Vlachogiannis, D., Sfetsos, A., and Nastos, P. T.: High-resolution dynamical downscaling of  
480 ERA-Interim temperature and precipitation using WRF model for Greece, 57, 799–825,  
481 <https://doi.org/10.1007/S00382-021-05741-9/FIGURES/17>, 2021.

482 Politi, N., Vlachogiannis, D., Sfetsos, A., Nastos, P.T., High resolution projections for extreme  
483 temperatures and precipitation over Greece, under review, <https://doi.org/10.21203/rs.3.rs-1263740/v1>,  
484 2022



485 Pongrácz, R., Bartholy, J., Gelybó, G., and Szabó, P.: Detected and expected trends of extreme climate  
486 indices for the carpathian basin, 15–28, [https://doi.org/10.1007/978-1-4020-8876-6\\_2](https://doi.org/10.1007/978-1-4020-8876-6_2), 2009.

487 Razieli, T., Daryabari, J., Bordi, I., Modarres, R., and Pereira, L. S.: Spatial patterns and temporal trends  
488 of daily precipitation indices in Iran, 124, 239–253, [https://doi.org/10.1007/S10584-014-1096-](https://doi.org/10.1007/S10584-014-1096-1/TABLES/1)  
489 [1/TABLES/1](https://doi.org/10.1007/S10584-014-1096-1/TABLES/1), 2014.

490 Rockel, B., Will, A., and Hense, A.: The regional climate model COSMO-CLM (CCLM), 17, 347–348,  
491 <https://doi.org/10.1127/0941-2948/2008/0309>, 2008.

492 Sadegh, M., Moftakhari, H., Gupta, H. v., Ragno, E., Mazdiyasi, O., Sanders, B., Matthew, R., and  
493 AghaKouchak, A.: Multihazard Scenarios for Analysis of Compound Extreme Events, 45, 5470–5480,  
494 <https://doi.org/10.1029/2018GL077317>, 2018.

495 Samuelsson, P., Jones, C. G., Willén, U., Ullerstig, A., Gollvik, S., Hansson, U., Jansson, C.,  
496 Kjellström, E., Nikulin, G., and Wyser, K.: The Rossby Centre Regional Climate model RCA3: model  
497 description and performance, 63, 4–23, <https://doi.org/10.1111/J.1600-0870.2010.00478.X>, 2016.

498 Schepsmeier, U., Stoeber, J., Christian, E., and Maintainer, B.: Package “VineCopula” Type Package  
499 Title Statistical inference of vine copulas, 2013.

500 Schwarz, G.: Estimating the Dimension of a Model, <https://doi.org/10.1214/aos/1176344136>, 6, 461–  
501 464, <https://doi.org/10.1214/AOS/1176344136>, 1978.

502 Singh, H., Najafi, M. R., and Cannon, A. J.: Characterizing non-stationary compound extreme events in  
503 a changing climate based on large-ensemble climate simulations, 56, 1389–1405,  
504 <https://doi.org/10.1007/S00382-020-05538-2/FIGURES/6>, 2021.

505 Sklar and M.: Fonctions de repartition a n dimensions et leurs marges, 8, 229–231, 1959.

506 Spiridonov, V., Somot, S., and Déqué, M.: ALADIN-Climate: from the origins to present date, n.d.

507 Tavakol, A., Rahmani, V., and Harrington, J.: Probability of compound climate extremes in a changing  
508 climate: A copula-based study of hot, dry, and windy events in the central United States, 15, 104058,  
509 <https://doi.org/10.1088/1748-9326/ABB1EF>, 2020.

510 Tošić, I. and Unkašević, M.: Extreme daily precipitation in Belgrade and their links with the prevailing  
511 directions of the air trajectories, 111, 97–107, <https://doi.org/10.1007/S00704-012-0647-5/FIGURES/9>,  
512 2013.

513 Tringa E and Kostopoulou E: An observational study of the relationships between extreme temperature  
514 and precipitation and the surface atmospheric circulation in Greece, n.d.

515 Trujillo, E., Molotch, N. P., Goulden, M. L., Kelly, A. E., and Bales, R. C.: Elevation-dependent  
516 influence of snow accumulation on forest greening, 5, 705–709, <https://doi.org/10.1038/ngeo1571>,  
517 2012.

518 Vajda, A., Tuomenvirta, H., Juga, I., Nurmi, P., Jokinen, P., and Rauhala, J.: Severe weather affecting  
519 European transport systems: The identification, classification and frequencies of events, 72, 169–188,  
520 <https://doi.org/10.1007/S11069-013-0895-4/TABLES/3>, 2014.

521 van Meijgaard, E., van Ulft, L. H., van de Berg, W. J., Bosveld, F. C., van den Hurk, B. J. J. M.,  
522 Lenderink, G., and Siebesma, A. P.: The KNMI regional atmospheric climate model RACMO version  
523 2.1, 2008.

524 Vogel, J., Paton, E., and Aich, V.: Seasonal ecosystem vulnerability to climatic anomalies in the  
525 Mediterranean, 18, 5903–5927, <https://doi.org/10.5194/BG-18-5903-2021>, 2021.

526 Voudouri, A. and Kotta, D.: Factors Determined Snow Accumulation Over the Greater Athens Area  
527 During the Latest Snowfall Events, 355–361, [https://doi.org/10.1007/978-3-642-29172-2\\_50](https://doi.org/10.1007/978-3-642-29172-2_50), 2013.

528 Wu, X., Hao, Z., Hao, F., and Zhang, X.: Variations of compound precipitation and temperature  
529 extremes in China during 1961–2014, *Science of The Total Environment*, 663, 731–737,  
530 <https://doi.org/10.1016/J.SCITOTENV.2019.01.366>, 2019.

531 Zanocco, C., Boudet, H., Nilson, R., Satein, H., Whitley, H., and Flora, J.: Place, proximity, and  
532 perceived harm: extreme weather events and views about climate change, 149, 349–365,  
533 <https://doi.org/10.1007/S10584-018-2251-X/TABLES/2>, 2018.

534 Zhang, W., Luo, M., Gao, S., Chen, W., Hari, V., and Khouakhi, A.: Compound Hydrometeorological  
535 Extremes: Drivers, Mechanisms and Methods, 9, 941,  
536 <https://doi.org/10.3389/FEART.2021.673495/BIBTEX>, 2021.

537 Zscheischler, J. and Seneviratne, S. I.: Dependence of drivers affects risks associated with compound  
538 events, 3, [https://doi.org/10.1126/SCIADV.1700263/SUPPL\\_FILE/1700263\\_SM.PDF](https://doi.org/10.1126/SCIADV.1700263/SUPPL_FILE/1700263_SM.PDF), 2017.

539 Zscheischler, J., Orth, R., and Seneviratne, S. I.: Bivariate return periods of temperature and  
540 precipitation explain a large fraction of European crop yields, 14, 3309–3320,  
541 <https://doi.org/10.5194/BG-14-3309-2017>, 2017.

542 Zscheischler, J., Westra, S., van den Hurk, B. J. J. M., Seneviratne, S. I., Ward, P. J., Pitman, A.,  
543 AghaKouchak, A., Bresch, D. N., Leonard, M., Wahl, T., and Zhang, X.: Future climate risk from  
544 compound events, 8, 469–477, <https://doi.org/10.1038/s41558-018-0156-3>, 2018.

545 Zhou, S., Zhang, Y., Williams, A. P., and Gentine, P.: Projected increases in intensity, frequency, and  
546 terrestrial carbon costs of compound drought and aridity events, *Science Advances*, 5,  
547 [https://doi.org/10.1126/SCIADV.AAU5740/SUPPL\\_FILE/AAU5740\\_SM.PDF](https://doi.org/10.1126/SCIADV.AAU5740/SUPPL_FILE/AAU5740_SM.PDF), 2019.

#### 548 **Code and data availability**

549 Code and results data available upon request.

#### 550 **Author contributions**

551 IM has worked on conceptualization, methodology, validation, visualization, investigation, writing  
552 review and editing. AS, DV and IK contributed on conceptualization, review and supervision. All  
553 authors have read and agreed to the published version of the manuscript.

#### 554 **Competing interests**

555 The authors declare that they have no conflict of interest.

556

#### 557 **Appendix**

NUMBER	LOCATION	ID	LATITUDE	LONGITUDE	ELEVATION (m)	YEARS
1	Alexandroupoli	16627	40.85	25.917	4	1980-2004
2	Elliniko	16716	37.8877	23.7333	10	1980-2004
3	Ioannina	16642	39.7	20.817	483	1980-2004
4	Irakleio	16754	35.339	25.174	39	1980-2004
5	Kalamata	16726	37.067	22.017	6	1980-2004

6	Kastoria	16614	40.45	21.28	660.95	1980-2004
7	Kerkira	16641	39.603	19.912	1	1980-2004
8	Kithira	16743	36.2833	23.0167	167	1980-2004
9	Larisa	16648	39.65	22.417	73	1980-2004
10	Limnos	16650	39.9167	25.2333	4	1980-2004
11	Methoni	16734	36.8333	21.7	34	1980-2004
12	Milos	16738	36.7167	24.45	183	1980-2004
13	Mitilini	16667	39.059	26.596	4	1980-2004
14	Naxos	16732	37.1	25.383	9	1980-2004
15	Rhodes	16749	36.42896	28.21661	95	1980-2004
16	Samos	16723	37.79368	26.68199	10	1980-2004
17	Skyros	16684	38.9676	24.4872	12	1980-2004
18	Souda	16746	35.4833	24.1167	151	1980-2004
19	Thessaloniki	16622	40.517	22.967	2	1980-2004
20	Tripoli	16710	37.527	22.401	651	1980-2004
21	Zakinthos	16719	37.751	20.887	5	1980-2004
22	Florina	16613	40.78	21.43	619	1980-2002
23	Aktio	16643	38.919	20.772	2	1980-2004
24	Anchialos	16665	39.217	22.8	19	1980-2000
25	Lamia	16675	38.883	22.433	12	1980-2004
26	Andravida	16682	37.92	21.293	10	1980-2004
27	Patras	16689	38.25	21.733	2	1980-1999
28	Tanagra	16699	38.317	23.533	140	1980-2000
29	Chios	16706	38.333	26.133	5	1980-2000
30	Elefsis	16718	38.064	23.556	20	1980-2000

558

559 **Table A1: HNMS stations information.**

560

561

562

563

564